Supplementary material for Quasi-harmonic temperature dependent elastic constants: Applications to silicon, aluminum, and silver.

C. Malica[1] **and A. Dal Corso**[1,2]

[1]International School for Advanced Studies (SISSA),
Via Bonomea 265, 34136 Trieste (Italy).
[2]IOM-CNR 34136 Trieste (Italy).

E-mail: `cmalica@sissa.it`

February 2020

1. Grüneisen parameters

In Figure 1 we report the mode-Grüneisen parameters used for the thermal expansion (TE) (Eq. 14) calculation for silicon, aluminum, and silver, calculated along selected high symmetry lines in the Brillouin zone.

2. Temperature dependent elastic constant flow-chart

The calculation of the temperature dependent elastic constants (TDECs) within the QHA with the `thermo_pw` code is divided in two parts illustrated in Figure 2.

The first part (a) corresponds to the calculation of the C^T_{ijkl} as a function of the temperature for the reference geometries given in input. For each reference geometry all the strained geometries required for an elastic constant calculation are generated and phonons are computed for each strained configuration. All these calculations can be ran sequentially or in parallel. The parallelism underlying each phonon-dispersion calculation (see for instance: ICTP lecture notes **24**, 163 (2009) by R. di Meo *et al.*) is implemented in `thermo_pw` using images parallelization. Having the phonon frequencies of each strained geometry it is possible to compute, within the harmonic approximation, the thermodynamic quantities that depend from them (in particular the vibrational free energy of Eq. 10). Then the second derivatives of the free-energy with respect to strain $\tilde{C}^T_{ijkl}$ are computed at each temperature (Eq. 9) and the results are corrected for finite pressure effects in order to get the stress-strain ECs C^T_{ijkl} (Eq. 4): this in shown in the last block in the figure. A file with the $C^T_{ijkl}(T)$ is written for each reference geometry.

The second part (b) is devoted to the computation of the anharmonic properties within the quasi-harmonic approximation. It needs the files of the $C^T_{ijkl}(T)$ at each reference geometry produced by the first part (a). The setup of the references geometries must be the same as in part (a). Phonons are computed at each reference geometry. This allows to compute the vibrational free-energy of each reference geometry. For each temperature T, the vibrational free-energy is added to the energy

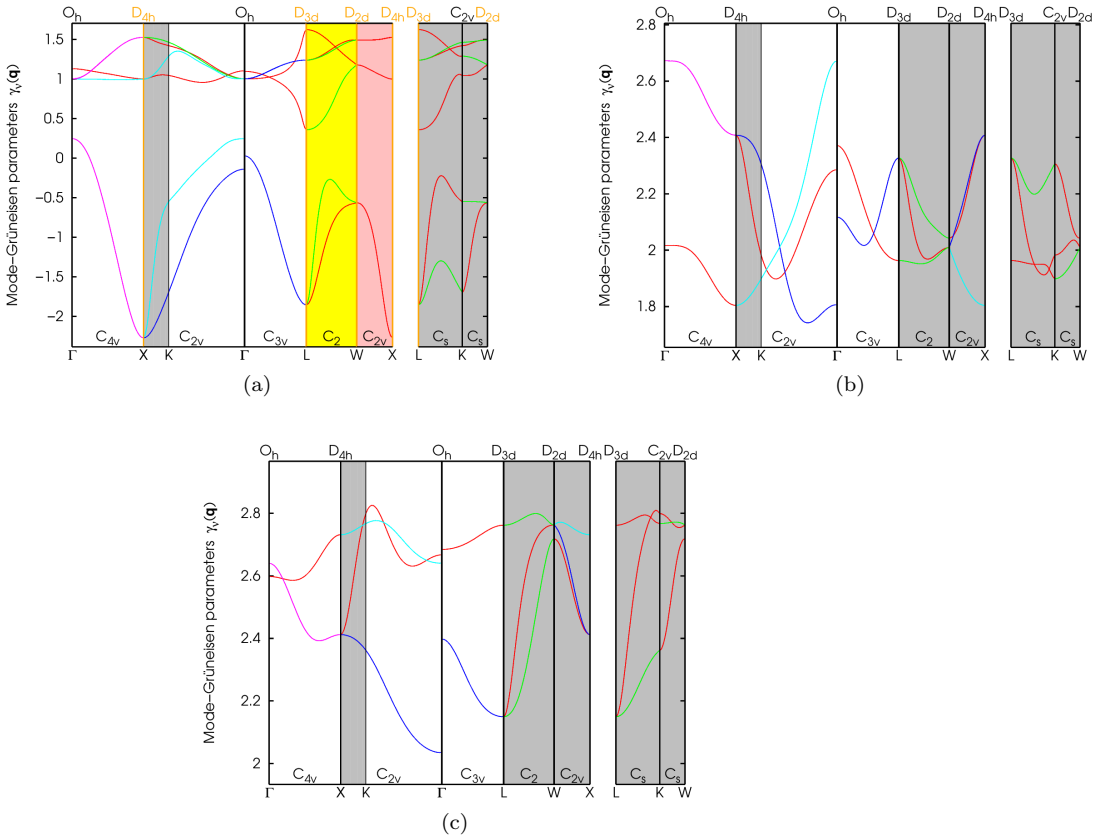

Figure 1: Mode-Grüneisen parameters for: a) silicon, b) aluminum, c) silver.

to get the Helmholtz free energy of the solid at the reference geometries. The free-energies at the various geometries are interpolated by a polynomial (the order of the polynomial can be varied) and minimized to obtain $a(T)$. The isothermal $C^T_{ijkl}(T)$ at the various geometries are interpolated by a polynomial and, at each temperature T, the value corresponding to $a(T)$ is evaluated from the polynomial interpolation: in this way we obtain the final QHA TDECs. Then, starting from this isothermal QHA TDECs, the adiabatic QHA TDECs, elastic compliances and bulk modulus are derived. In this second part the parallellization is done as in the first part as shown in Figure 2 although the number of required phonon dispersions is much smaller than in the first part. In order to compute the free-energy as a function of the strain we used in the first part an even number (6 values) of strains centered around $\epsilon = 0$. However this point is not included. If the user select an odd number of strained configurations then the central geometry is considered. In this case the user can use the dynamical matrices already computed for the reference $\epsilon = 0$ geometry to run the second part of the calculation.

In order to compute the TDECs within the QSA, the ECs are computed at $T = 0$ K at the different reference geometries by using the stress-strain relation (Eq. 2) or the second derivatives of the total energy (Eq. 3 and Eq. 4) and then they are saved on a different file for each geometry. Part (b) does not change provided that the files

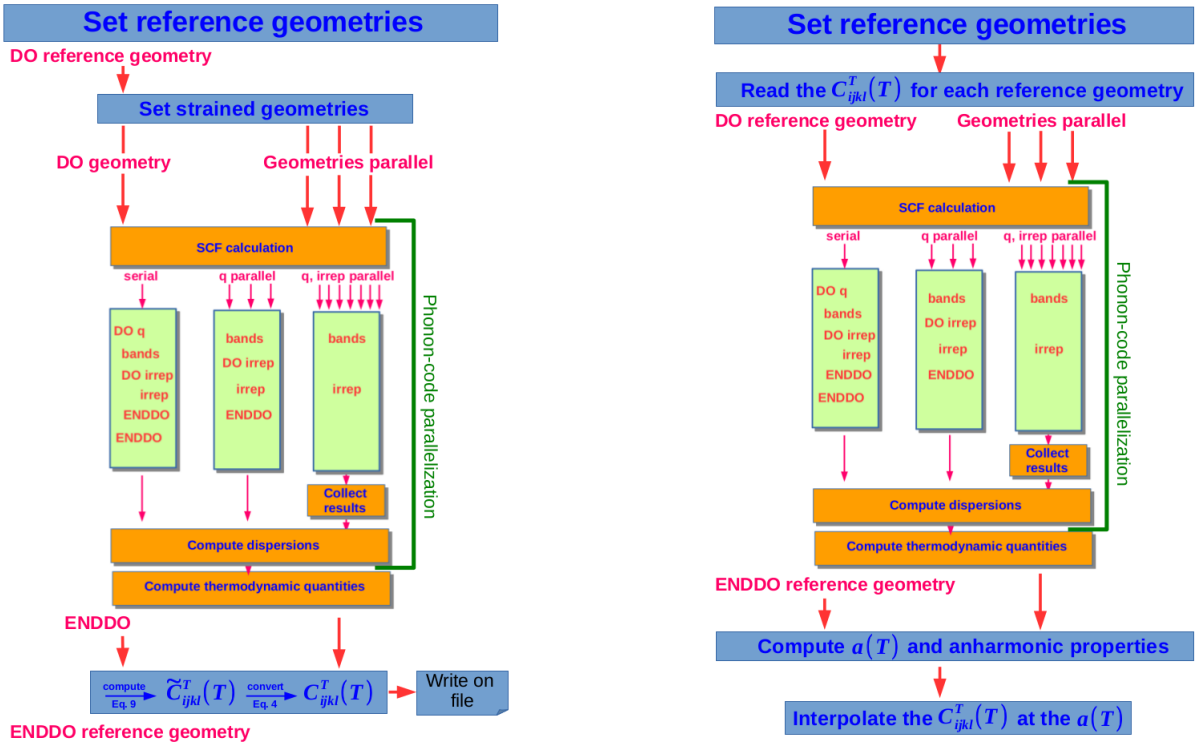

Figure 2: Flow-chart of the calculation of the TDECs within the QHA with the `thermo_pw` code.

of the $T = 0$ K ECs are read instead of the $C^T_{ijkl}(T)$.

3. Some tests: elastic constants at $T = 0$ K

Some tests of the ECs calculation by using the `thermo_pw` code can be found in Ref. [21]. In this section we investigate a few other examples. As in Ref. [4] we considered In, TiO_2 rutile, and Al_2O_3 and computed the ECs at $T = 0$ K from the second derivatives of the total energy with respect to strain (Eq. 3 of the paper), after minimizing the total energy with respect to the crystal parameters and finding the equilibrium geometry. We also verified the result computing the ECs from the stress-strain relation (Eq. 2 of the paper). Both methods are available in the code. Moreover, we computed some properties of macroscopic elasticity as described in the tables captions. In these tables we compare our results with those obtained in Ref. [4] and with the experimental data reported in the same paper.

3.1. Indium

We used the Wu-Cohen (WC) exchange-correlation functional (Z. Wu, R.E. Cohen, Phys. Rev. B **73**, 235116, 2006) and the pseudopotential

Table 1: Elastic properties of indium. Crystal parameters are in units of the Bohr radius. The elastic constants C_{ij} are in kbar. Bulk modulus B (kbar), shear modulus S (kbar) and Young's modulus Y (kbar) and Poisson's ratio V are calculated within the Voigt (V) and Reuss (R) approximations. The average of the two according to the Voigt-Reuss-Hill (H) method is also reported. Transverse elastic wave velocity v_t, longitudinal elastic wave velocity v_l and the average wave velocity v_m are reported in m/s and the Debye temperature Θ_D in K.

	This work	Other theoretical	Expt.
Method	PAW-PP	FP-LAPW	
Functional	WC	WC	
a_0	6.0956	6.0491	6.1439
c_0	9.3414	9.4324	9.3479
C_{11}	617	589	525
C_{12}	302	332	368
C_{13}	424	374	371
C_{33}	500	448	530
C_{44}	70	58	78
C_{66}	54	25	147
B_V	448	421	422
B_R	448	414	422
B_H	448	418	422
S_V	78	65	92
S_R	62	50	86
S_H	70	57	89
Y_V	220	185	257
Y_R	178	143	242
Y_H	199	164	250
V_V	0.418	0.426	0.398
V_R	0.434	0.442	0.404
V_H	0.425	0.434	0.401
v_t	971	875.2	1105.2
v_l	2702	2573.2	2723.6
v_m	1103.1	995.4	1251.4
Θ_D	109	100.6	125.5

`In.wc-dn-kjpaw_psl.1.0.0.UPF` from `pslibrary`. The cutoff for the wave functions was 70 Ry, the one for the charge density 500 Ry, the **k**-point mesh was $48 \times 48 \times 32$. The presence of the Fermi surface has been dealt with by the MP [41] smearing technique with a value of the smearing parameter $\sigma = 0.02$. The equilibrium configuration was obtained by interpolating the total energy computed in a 5×5 grid of a and c/a crystal parameters with a 2-dimensional fourth-degree polynomial and by minimizing it ($\Delta a = 0.05$ a.u., $\Delta(c/a) = 0.02$). The results are reported in Table 1.

3.2. Rutile TiO_2

We used the Perdew-Burke-Ernzerhof (PBE) exchange-correlation functional (J. P. Perdew *et al.*,, Phys. Rev. Lett. **77**, 3865, 1996) and the pseudopoten-

Table 2: Elastic properties of rutile TiO_2. Crystal parameters are in units of the Bohr radius. The elastic constants C_{ij} are in kbar. Bulk modulus B (kbar), shear modulus S (kbar) and Young's modulus Y (kbar) and Poisson's ratio V are calculated within the Voigt (V) and Reuss (R) approximations. The average of the two according to the Voigt-Reuss-Hill (H) method is also reported. Transverse elastic wave velocity v_t, longitudinal elastic wave velocity v_l and the average wave velocity v_m are reported in m/s and the Debye temperature Θ_D in K.

	This work	Other theoretical	Expt.
Method	PAW-PP	FP-LAPW	
Functional	PBE	PBE	
a_0	8.7860	8.6809	8.6806
c_0	5.6138	5.5900	5.5911
C_{11}	2566	2683	2690
C_{12}	1677	1802	1770
C_{13}	1465	1464	1460
C_{33}	4693	4779	4800
C_{44}	1148	1223	1240
C_{66}	2111	2236	1920
B_V	2116	2178	2173
B_R	2012	2094	2086
B_H	2064	2136	2130
S_V	1229	1298	1246
S_R	947	978	986
S_H	1088	1138	1116
Y_V	3090	3248	3138
Y_R	2456	2538	2556
Y_H	2773	2898	2851
V_V	0.257	0.251	0.259
V_R	0.297	0.298	0.295
V_H	0.274	0.273	0.276
v_t	5133.0	5174.2	5125.8
v_l	9224.5	9272.1	9228.0
v_m	5716.2	5760.8	5709.0
Θ_D	754.7	785.6	778.5

tials `Ti.pbe-spn-kjpaw_psl.1.0.0.UPF` and `O.pbe-nl-kjpaw_psl.1.0.0.UPF` from `pslibrary`. The cutoff for the wave functions was 50 Ry, the one for the charge density 350 Ry, the **k**-point mesh was $12 \times 12 \times 20$. The equilibrium configuration was obtained by interpolating the total energy computed in a 5×5 grid of a and c/a crystal parameters with a 2-dimensional fourth-degree polynomial and by minimizing it ($\Delta a = 0.05$ a.u., $\Delta(c/a) = 0.02$). The results are reported in Table 2.

3.3. Rhombohedral Al_2O_3

We used the Perdew-Burke-Ernzerhof (PBE) exchange-correlation functional and the pseudopotentials `Al.pbe-nl-kjpaw_psl.1.0.0.UPF` and `O.pbe-n-kjpaw_psl.1.0.0.UPF` from `pslibrary`. The cutoff for the wave functions was 70 Ry, the one for the charge

Table 3: Elastic properties of rhombohedral Al_2O_3. Crystal parameters are in units of the Bohr radius. The elastic constants C_{ij} are in kbar. Bulk modulus B (kbar), shear modulus S (kbar) and Young's modulus Y (kbar) and Poisson's ratio V are calculated within the Voigt (V) and Reuss (R) approximations. The average of the two according to the Voigt-Reuss-Hill (H) method is also reported. Transvers elastic wave velocity v_t, longitudinal elastic wave velocity v_l and the average wave velocity v_m are reported in m/s and the Debye temperature Θ_D in K.

	This work	Other theoretical	Expt.
Method	PAW-PP	FP-LAPW	
Functional	PBE	PBE	
a_0	9.0924	9.0928	8.9916
c_0	24.8081	24.8253	24.5498
C_{11}	4516	4656	4974
C_{12}	1510	1383	1640
C_{13}	1091	1036	1122
C_{33}	4537	4588	4991
C_{44}	1319	1363	1474
C_{14}	−200	−24	−236
B_V	2328	2312	2523
B_R	2325	2308	2518
B_H	2326	2310	2521
S_V	1487	1569	1660
S_R	1443	1547	1606
S_H	1465	1558	1633
Y_V	3677	3838	4084
Y_R	3587	3793	3974
Y_H	3632	3816	4029
V_V	0.237	0.223	0.230
V_R	0.242	0.226	0.236
V_H	0.240	0.224	0.233
v_t	6160.5	6355.4	6399.3
v_l	10529.9	10665.7	10853.7
v_m	6831.3	7035.3	7090.9
Θ_D	979.4	1015.3	1034.8

density 500 Ry, the **k**-point mesh was $12 \times 12 \times 12$. The equilibrium configuration was obtained by interpolating the total energy computed in a 5×5 grid of the lattice constant a and angle α with a 2-dimensional fourth-degree polynomial and by minimizing it ($\Delta a = 0.05$ a.u., $\Delta\alpha = 0.5$). The results are reported in Table 3.

4. Thermoelasticity of MgO

In this section we compare the results obtained by our approach with the QHA TDECs of MgO available in the literature in Refs. [9, 10] cited in the paper. This example is also useful to test a material with ionic bonds, since in the main paper we considered only covalent and metallic systems.

In order to minimize as much as possible the differences between our calculation and the literature, we used the LDA for the exchange-correlation energy and the norm-conserving pseudopotentials from the Quantum Espresso pseudopotentials library: `Mg.pz-n-vbc.UPF` and `O.pz-mt.UPF`. The cutoff for the wave functions was 90 Ry. The **k**-point mesh was $12 \times 12 \times 12$. Density functional perturbation theory (DFPT) was used to calculate the dynamical matrices on a $4 \times 4 \times 4$ **q**-point grid. These dynamical matrices have been Fourier interpolated on a $200 \times 200 \times 200$ **q**-point mesh to evaluate the free-energy. We used 9 reference geometries with lattice constants separated from each other by $\Delta a = 0.05$ a.u. and centered in the $T = 0$ K equilibrium lattice constant: 7.93 a.u.. In order to fit the free-energy as a function of strain we use a polynomial of degree two. To fit the ECs computed at the various reference configurations at the temperature dependent geometry we use a polynomial of degree three. In Fig. 3 we report the TDECs.

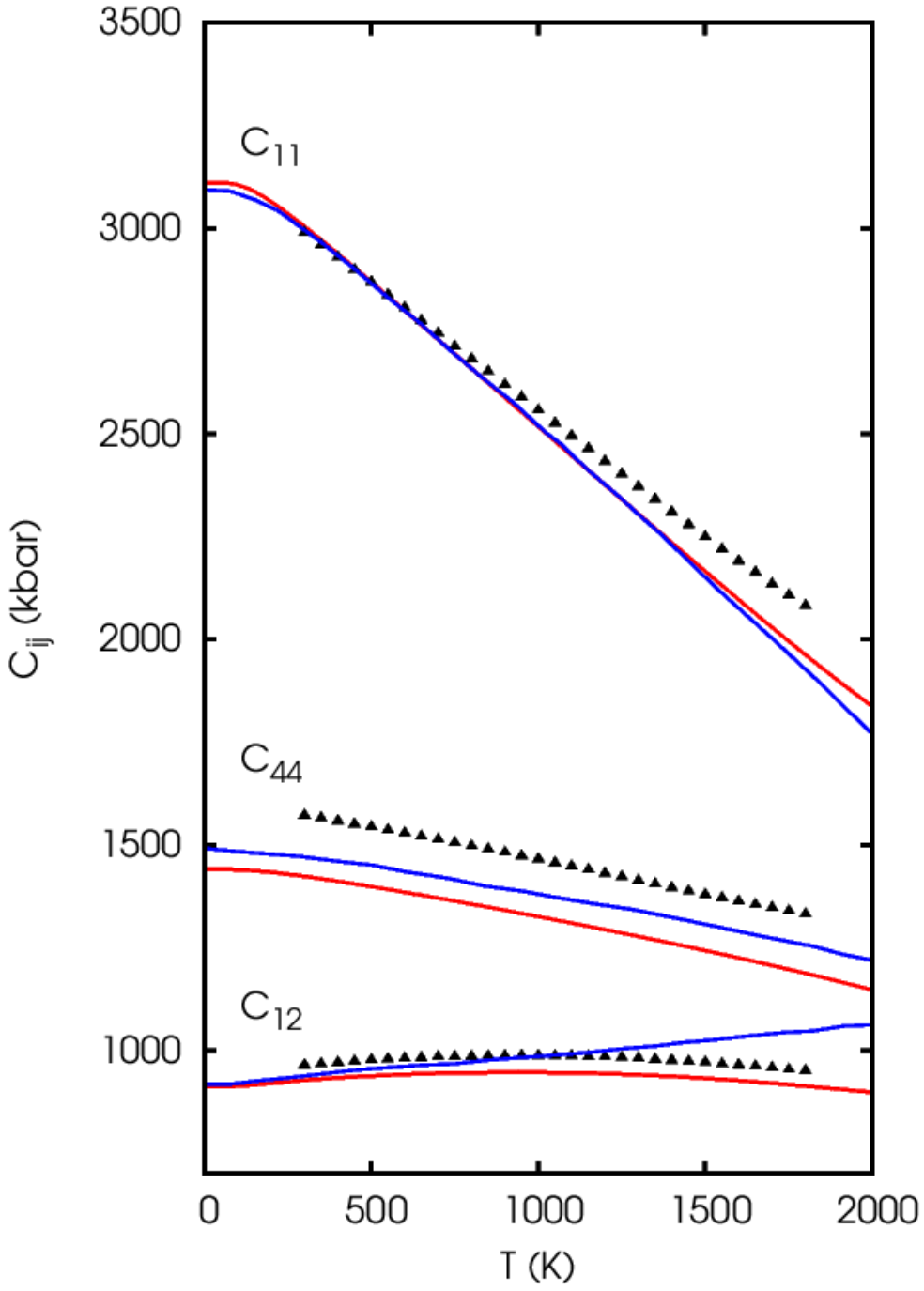

Figure 3: Adiabatic QHA TDECs of MgO. This work (red curves) compared with the results of Refs. [9,10] (blue curve). The points are experimental data, the same shown in [9,10].